International Journal of Communication Systems

WILEY

RESEARCH ARTICLE

Optimal Spectrum Sensing Framework for Cognitive Radio Networks Using Attention-Based Autoencoder With Multi-Scale Capsule Network

R. Koteswara Rao | Madona B. Sahaai

Department of ECE, VISTAS (Vels Institute of Science, Technology and Advanced Studies), Chennai, Tamil Nadu, India

Correspondence: R. Koteswara Rao (ravinutala814@gmail.com)

Received: 25 March 2025 | **Revised:** 13 September 2025 | **Accepted:** 1 October 2025

Keywords: adaptive and residual hybrid network | attention-based autoencoder with multi-scale capsule network | cognitive radio networks | optimal spectrum sensing | revised uniform variable-based addax optimization algorithm

ABSTRACT

Wireless communication industry's explosive growth over the last 10 years caused a shortage of resources since its demand has greatly increased. A technology called cognitive radio (CR) was created to make efficient utilization of the spectrum from radio sources. The effectiveness of CR is significantly influenced by the spectrum sensing (SS) function, and it is the primary function of CR, which helps to discover available spectrum for better spectrum utilization and reduce detrimental conflict with approved users. In addition, the conventional models cause high computational complexity in the SS. In this work, an adaptive SS system for CR networks is developed to identify unused bands of frequencies in order to get outside of these constraints. Initially, the essential synthetic data are gathered manually, and these data are used by the suggested adaptive and residual hybrid network (A-RHN) for SS. The A-RHN network is developed by using an attention-based Autoencoder with a multi-scale capsule network (AA-MCN). Moreover, the effectiveness of this model is enhanced by optimizing parameters via the revised uniform variable-based addax optimization algorithm (RUV-AOA). The proposed model enables more efficient use of the available spectrum by avoiding transmitting on frequencies that are already in use.

1 | Introduction

An emerging technique for mitigating the increased spectrum occupancy in telecommunications services is cognitive radio (CR) [1]. In order to address the shortage of frequency bands in the industrial and medical domains, the SS is proposed in wireless networks [2]. A CR uses a self-organized mechanism to implement flexible access to available network resources. In order to determine spectrum gaps and prevent disruption, SS approaches are used that estimate the available bandwidth availability of network resources [3]. It consists of small devices called secondary users (SU) that offer CR features and primary users (PU) that have inherited rights on spectrum usage, as well as a fusion center (FC) that combines the received data from SUs to make the ultimate decision regarding the availability of spectrum bands using SS [4, 5]. On the other hand, adding spectrum-detecting capabilities will force nodes to use more energy, which will shorten the network's lifespan.

The SS is necessary to exploit the spectrum efficiency of the CR. Effective use of the existing spectrum is more crucial because of the demand for wireless communications. Understanding certain frequency bands that are controlled by key users is crucial [6]. CR can use this information to decide whether these PU are active or not, which allows them to make recommendations about how to use the spectrum. SS results indicate that CR can temporarily use a frequency band when no PU is using it. This preserves the quality of the licensed spectrum by preventing interference [7]. Better use of available frequencies is made possible by monitoring and adjusting changes in the spectrum. This function enhances network performance in addition to optimizing resource usage. Additionally, CR can offer consumers an enhanced experience by lowering the likelihood of congestion and interference. The logical order of sensing decisions for calculating the occupancy patterns and PU activity statistics is the goal of SS [8]. The CR network can use this statistical information to predict future trends in spectrum occupancy, select the best spectrum band for maximizing system performance, and increase spectral effectiveness. In recent years, the academic community has paid close attention to the estimation of spectrum occupancy and PU activity statistics [9]. The researchers used a combination of the beta distribution to demonstrate a deterministic and stochastic model for spectrum occupancy [10, 11].

Classifying whether the PU exists is the fundamental idea behind SS. Few studies has been used deep learning techniques to handle SS as a classification problem. The SU mechanism can potentially sense the licensed bands to transmit the data without impacting the PUs overall process in the CRN technology. Also, it helps to enhance efficient and adaptive spectrum utilization and reduce the communication latency [12]. Spectrum detection using artificial neural networks (ANNs) is done on the CR. Energy values is employed as training features in a unique ANN-based hybrid sensing strategy [13]. Naïve Bayes classifier is used to sense the signal at a low SNR condition. Additionally, many studies have used the deep learning method for SS [14]. The deep learning frameworks use a shallow/deep multilayer perceptron network (MLP) for SS. This model is incompetent in storing data because it requires memory elements is a major drawback [15]. Therefore, time-series data and temporal modelling are not suitable matches for MLP. Conventional SS techniques frequently fail to detect a large variety of frequencies [16]. Because of this, these techniques do not perform well in complicated spectrum environments because they ignore variations in spectrum consumption brought by interference from nearby bands [17]. The conventional model provides a higher misclassification rate in the SS also causes inherent computational complexity. In this regard, the innovative model is proposed in this research for SS.

This research provided the following contributions in SS on the CR network.

- To exploit the optimal SS strategy in CR for diagnosing the availability of the frequency resources within the network. In addition, the instantaneous detection of the opportunistic white spaces, occupancy patterns, and PU's activity statistics are possibly determined using this suggested solution. Moreover, the frequency band currently utilized by the PU is determined using the recommended model, since this approach allows the SU to operate safely within the CR without interference by detecting the existence or absence of PU within the CR.
- To suggest the RUV-AOA in the A-RHN for tuning the hidden neuron and learning rate to enhance the accuracy and minimize the false omission rate (FOR) in SS operation. The RUV-AOA analyzes the historical data and adaptively explores the search space for maintaining the potential solution in the search process. In addition, the fast convergence properties of the RUV-AOA critically enhance the capability of the suggested model so that it can easily determine the unused frequency bands within the CR.
- To propose A-RHN for accurately detecting the unused spectrum in the CR. It helps to ensure the maximum utilization of the licensed spectrum for enhancing the transmission performance. The A-RHN is made up of a combination of MCN and AA to effectively perform the SS with high accuracy. The A-RHN model inherently recognizes the features in the data; also, this model weighs the different features over time to highlight the important patterns that contribute to detecting the presence of unused spectrum within the CR. The proposed SS operations are used for enhancing energy efficiency and minimizing the interference issues within the CR.

The following shows the structure of the model: In Section 2, the related works are clearly outlined. The system model and problem formulation for effective SS in CRN are given in Section 3. Section 4 explains the architecture of the proposed deep learning-based SS model. The presented network for efficient SS and its objective function are reported in Section 5. The simulation results are elaborated in Section 6. The final remarks are given in the Section 7.

2 | Literature Survey

2.1 | Related Works

In 2024, Almuqren et al. [18] have presented an optimal deep learning empowered malicious user detection for SS (ODL-MUDSS) in the CR. The automatic recognition and categorization of malicious users (MUs) was the primary goal. The ODL-MUDSS model outperformed other models, with a maximum accuracy.

In 2021, Kaschel et al. [19] have examined a novel framework for modelling dynamic CR in order to anticipate energy usage. The Kataoka criterion-based solution was offered to reduce the amount of energy used. It determined an ideal energy-efficient solution with a certain probability. To improve the exhaustive search approach, a reduced-complexity algorithm calculated the total number of active nodes. In dynamic scenarios, comprehensive simulation demonstrates the proper operation of the suggested approach.

In 2020, Soni et al. [20] have designed a long short-term memory (LSTM) network, which learned implicit characteristics from the spectrum data. To further improve CR efficiency, the advantage of the PU activity statistics was also adopted. Using spectral data from a variety of radio technologies, the recommended sensing systems were verified.

In 2024, Fouda and Fouda [21] have suggested three new statistical test-based techniques and blind autocorrelation and randomness tests. The second test was created using Bartlett's test and ANOVA. In order to reproduce the statistical characterization of genuine noise environments, Middleton Class A impulsive noise was also modelled. Modern SS approaches were employed in a number of comparison scenarios under low signal-to-noise ratio settings.

In 2021, Miah et al. [22] have developed a non-sequential technique to improve sensing gain in a CR-based Internet of Things (CR-IoT) network. The sequential approach assesses the degree of reliability to more efficiently assess SS. Prior to making a final choice, the hard decision fusion rule at the fusion center was adopted.

In 2021, Ye and Jiang [23] have designed an ideal linear weighted cooperative SS method in CR. Different weight values were allocated based on the historical sensing accuracy. Furthermore, the users with the best channel characteristics were chosen to collect local sensing data. According to simulation results, the suggested strategy can increase sensing performance and lower the likelihood of inaccuracy.

In 2024, Ezhilarasi and Clement [24] have presented energy detection-based SS and blockchain-based MU detection with SHA-3 hashing. Here, two different stages were utilized to the identification strategy: the block update phase and the iron-out phase. Consequently, it has been demonstrated that the CR blockchain network's privacy has greatly increased.

In 2024, Vijay and Aparna [25] have presented a convolution neural network-transformer network (CNN-TN)-based spectrum method that combines both CNNs and TNs for SS. CNNs can identify key features from spectrum data. However, TN has the capacity to optimize these properties. This technique captures both local and global patterns resulting in minimal sensing errors and a higher likelihood of detection. Additionally, the outcomes imply that actual wireless communications systems might use this model to enhance their effectiveness.

In 2025, Yao et al. [26] have proposed an alternating optimization (AO) to derive a closed-form expression for the CRN's detection threshold optimally. Also, the received beamforming and the antenna positions at the SU have been significantly addressed with the help of a closed-form solution. Further, the fluid antenna locations could be recognized by utilizing the successive convex approximation (SCA), and the simulation analysis was implemented in the validation process to provide significant improvements than the conventional methods.

In 2024, Roopa and Pradhan [27] have proposed a novel deep learning-oriented SS (DLoSS) approach with the help of deep neural networks (DNNs) for cooperative spectrum sensing (CSS) mechanisms. Then, the prescribed informative features such as hidden spatial and temporal data from the incoming modulated signals were significantly extracted to maximize the detection performance.

In 2025, Taherpour et al. [28] have proposed a novel framework for accurately estimating the covariance matrix in the sample covariance matrix based on linear spectral statistics theory. It has the ability to timely validate the significant antenna and sample numbers influence the proper outcomes. Also, the simulation results illustrate the efficiency of the developed method in various large array antenna networks; thus, it proves its notable benefits than the conventional methods.

In 2024, Ambhika [29] has proposed a support vector machine (SVM) for enhancing the performance of SS mechanism to significantly detect the malicious user by randomly choosing the PU and SU. Here, the Bayesian optimization algorithm (BOA) was utilized in the optimization process to significantly tune the hyperparameters of SVM for enhancing the detection phase and the convergence speed. At last, the experimental validation proves the proposed approach's superior performance.

In 2025, Mochigar and Matad [30] have proposed an improved quantum inspired evolution (IQISE) algorithm with residual network 50 (ResNet50) mechanism to efficiently mitigate the SS and utilization-related issues in CRN. It has the ability to improve the training and the optimization process; also, the experimental outcomes show the proposed approach's truthful performance.

2.2 | Problem Statement

One of the vital processes in the CR is SS. The development of wireless communication applications is restricted because of the lack of available resources. The best available channel is utilized by the CR to get rid of spectrum congestion interferences in the intelligently programmed CR. The unused band in the intelligent radio is determined by the core technique called as SS, and this approach is determined by the presence or absence of the PU by continually monitoring the frequency band. Table 1 shows the uses and limitations of the existing model.

- The conventional ODL-MUDSS approach [18] is more sensitive for efficiently distinguishing a faded and shadowed primary signal in a larger network space, which may wrongly interpret the primary system. Here, the SS performance is affected due to the uncertainty of aggregate interference thus; it enhances the possibility of multiple CRN operating at the same licensed band, making overfitting issue. Also, the changing CR environment is not adapted by this model, and it is not effective for dealing with the fades, interference, and noise within the CR. Here, the proposed model can effectively adjust the variation in the signal characteristics of CR. Thus, it helps to optimally handle vast amount of faded and shadowed primary signals in a larger network space to reduce the overfitting and underfitting complexities in the training performance.

- The noise uncertainty issues within the CR are not effectively solved by the conventional LSTM-SS model [20], and it consumes more hardware requirements for the implementation. Further, it needs a longer sensing duration to attain a desired performance level, and its inability to discriminate among received energy sources leads to uncertainties in background noise. More sophisticated feature extractors are needed to capture the primary signal's carrier frequency, leading to higher complexity and inaccurate detection. Here, A-RHN is developed for SS performance that can handle the noise uncertainty issues and it requires low hardware requirements. Also, it consumes minimal computational

TABLE 1 | Features and challenges of the conventional SS models in CR.

Author [citation]	Methodology	Features	Challenges
Almuqren et al. [18]	ODL-MUDSS	The threat flagged inside the network is detected by this model.	It has a high prediction error in the operation of SS.
Kaschel et al. [19]	Kataoka criterion	The probability of the energy spent on the network is identified by this work.	The dynamics of the sensor nodes are effectively handled using this model.
Soni et al. [20]	LSTM-SS	Implicit features from the spectrum data are learned by this model.	The SS for multiple PU and SU is not attained by this model.
Fouda and Fouda [21]	ANOVA	The SS in the congested network is performed by this model.	The probabilities of the noise are not detected by this model.
Miah et al. [22]	Sequential approach	The global error probability of the model is very low and the expected lifetime of the network is enhanced by this model.	The sensing gain and throughput are not improved using this model.
Ye and Jiang [23]	Optimal linear weighted cooperative SS	The historical sensing accuracy of the model is very high.	The error probability of the model is very high.
Ezhilarasi and Clement [24]	SHA-3 algorithm	It significantly enhances the security of the cognitive blockchain technology and the integrity of the data within the system is enhanced using this model.	The robustness of the model is very low.
Vijay and Aparna [25]	CNN-TN	Better probability and lower sensing error is attained by this model.	It takes more time to capture the local and global patterns in the spectrum data.

duration for achieving better SS detection performance, making better decision making in an efficient manner.

- The conventional sequential [22] method is limited for optimally validating the sensing interference duration and location of the receiver, due to the presence of unlicensed users. It is not capable of continuously monitoring and updating the condition of the PU's channel's interference temperature level and transmission duration, resulting in imbalanced accuracy and high computational complexity. Here, the hybrid model with optimal tuning is proposed that can effectively balance the computational efficiency and accuracy in the SS.
- The conventional CNN-TN approach [25] does not discover the existence of absence of PUs and does not reduce the irrelevant noises from the data to maximize the overfitting issues. In the optimization phase, it is ineffective for significantly tuning the parameters to gradually enhance the vanishing-gradient complexities. Here, the optimized RUV-AOA model is proposed to ultimately tune the prescribed parameters in the RHN approach for improving the overall detection performance, and it is specially tailored for solving the SS issues involved in the large CRN space.
- The prior SVM model [29] is not suitable for preventing the collision between the SU and PU in the CR, so they did not predict the availability of the spectrum within the CR. Here, the multiscale model is proposed that predicts the collision between the PU and SU for attaining the accurate SS in the CR without any interference, and it has the ability to efficiently reduce the vanishing gradient complexities.

3 | System Model and Problem Formulation for Effective SS in CRN

3.1 | Cognitive Radio Networks: System Model

This research suggests the SS technique to enhance sensing efficiency and lower the error risk of decision fusion. It is anticipated that CR is aware of the communication state between the FC. Prior to transmitting sensing data at each interval, the channel status must be estimated. Furthermore, the most nearby cognitive users ought to be chosen as membership nodes in the same cluster in the node's clustering structure, and the state of the channel may be roughly considered to be optimum. Cluster heads (CHs) will ultimately forward the fusion results from each cluster to the FC, which are analyzed using the fusion procedure [23]. In the SS, the FC and cognitive user O participate. The cluster L is formed by organizing the SU. In the cluster d, totally l_d number of cognitive users is available. At the sampling slot n and the cluster d, the SS sample of the j^{th} SU is attained by applying the energy detection method, and it is given in Equation (1).

$$s_{dj}(n) = \begin{cases} o_{dj}(n) & I_0 \\ i_{dj}t_{dj}(n) & I_1 \end{cases} \tag{1}$$

The PU's signal received by the SU has the sampling value of $s_{dj}(n)$, and the channel gain is represented as i_{dj}. From the SU to PU, the channel noise is represented as $o_{dj}(n)$. The system model of the CR is visualized in Figure 1.

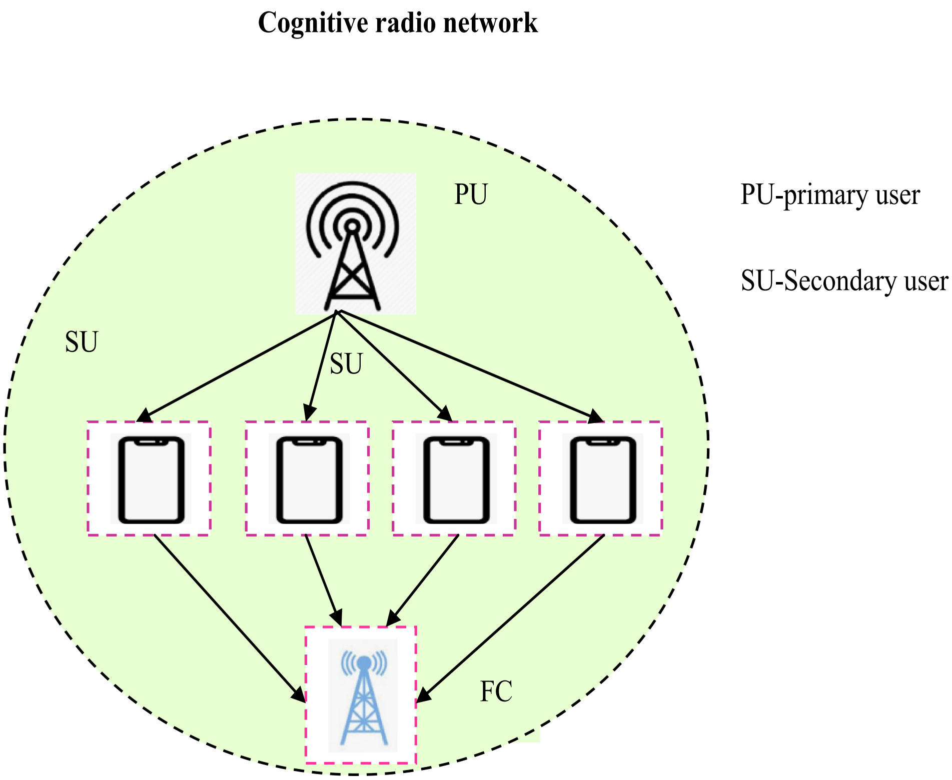

FIGURE 1 | System model of the CR.

3.2 | Problem Formulation

The energy consumption is the greatest issue associated with the SS in CR. Two states of categories are comprised in the SS, and the SS problem is formulated as the binary classification problem. If the primary user (PU) is present, then the channel is classified as idle. When the PU is absent, then the channel is available in the occupied state [25].

$$\{P_j\} = \begin{cases} I_0: \{\lambda_j\} \\ I_1: \{N_j + \lambda_j\} \end{cases} \tag{2}$$

The received sample is represented as P, the in-phase and quadrature-phase elements are represented by the matrix 128×2, the term j is another attribute lies in between $[1, V]$, phase quadrature phase format is available with the size of 128×2, the modulation signal of the PU is N, and the noise signal is represented as λ. The hypothesis I_1 is selected when the PU is present; otherwise, the hypothesis I_0 is selected. The number of samples taken for the modulation is denoted as V. The missing probability detection $Q_{ne} = Q\{I_0 | I_1\}$ and the presence of the noise in the signal are determined by channel activity, and it is given in Equation (3).

$$\begin{pmatrix} p \\ l \end{pmatrix} = \begin{cases} p_1 & p_2 & p_3 & p_4 & p_5 & p_a \\ l_1 & l_2 & l_3 & l_4 & l_5 & l_a \end{cases} \tag{3}$$

Here, the label value is denoted as l, and the modulation signal in the noise is represented as o.

3.3 | Synthetic Dataset Generation

The process of creating artificial data that resemble the features of real-world data is called synthetic dataset generation. Here, the equal representation of the PU signal and Gaussian noised representation are adopted in the generation of the synthetic data. In the synthetic data generation, the new sensory data are synthesized, which plays a crucial role in optimal spectrum sensing process. The developed model will be trained using the synthetically generated data, which helps to enhance the generalization capability of the developed model. The condition of the CR is varied based on the interference, behavior of the user, and environmental factors. The synthetically generated data can have the capability to handle the condition of the CR systematically and often solve the challenges involved in the SS. The syntactically generated data are gathered from the link of https://github.com/caiotavares/spectrum-sensing with access date: 2025-02-05.This dataset contains four folders and the code available in this resource master's degree in electrical engineering. The term Q_l denotes the data collected from the sources and $l = 1, 2 \ldots L$; here, the term L denotes the total quantity of the synthetically collected data.

4 | Architecture of the Proposed SS Model

4.1 | Structural Description of the Proposed Approach

The increased spectrum occupancy of the telecommunication services is overcome by the CR. The scarcities of the frequency band in various industries are solved using this paradigm. The spectrum resources are widely managed with the incorporation of the CR. In an environment with low SNR, the conventional approaches do not detect the PU with the CR. This model has a higher false alarm rate and provides missed SS results because they are not suited for differentiating the actual and noisy signals in the CR. The rapid variation in the spectrum usage is not adopted by the conventional models, and the highly dynamic nature of the wireless spectrum makes the SS process as complex task. In addition, the temporal correlation in the spectrum usage data is not attained by the conventional models. Despite these challenges, this research leads to the development of an innovative model for enhancing the SS in the CR. The prior deep learning model provides higher computational complexity and misclassification rate in the SS. The overall view of the proposed model is given in the Figure 2.

As a solution to the challenges of the conventional models, this research investigated an innovative model for SS to detect the unused bands within the CR with the aim of detecting the presence or absence of the PU in the CR. The suggested model cannot disturb the PU while accessing the underutilized bands within the CR. The designed SS system avoids interference issues by detecting the availability of the resources in terms of bandwidth spectrum holes and so forth. This system is more helpful for increasing the transmission opportunities in the CR. Moreover, the immediate detection of the opportunistic white spaces in the CR is also performed using the proposed solution, and it provides the interweave communication between the PU and SU in the CR. The determination of when the PU vacates their licensed spectrum in the CR is made during the process of SS using the proposed solution so that the same band is broadcasted by the SU within the CR. The effective transmission in the CR is possible by the proposed model as it accurately senses the absence of the PU for confirming the maximum utilization of the licensed spectrum in the CR. This model enhances the accuracy of the SS by handling the uncertainty, shadowing, and fading effects in CR. The data required for the process of the SS are synthetically generated, and these synthetically generated data are used for effectively training the developed model in the SS operation. In addition, the training of deep learning models using synthetically generated data helps to learn the underlying patterns in the data. Further, the A-RHN is used for performing the SS operation within the CR. The A-RHN is an efficient model made up of two structures such as an attention-based autoencoder and a multi-scale capsule network for effectively performing the SS operation. The critical features of the input data are encapsulated by the autoencoder. The high dimensional data encountered in the SS problem are effectively managed by this model. It is better to capture the long-range dependencies of the data by utilizing the attention mechanism with the proposed model. The specific features in the input data with different hierarchies are attained with the help of the capsule network. The feature regardless of this transformation is captured because of the inherent capability of the CapsNet model; thus, the generalization performance of the CapsNet is improved and provides ultimate results in the SS. The multiscale module within the CapsNet leverages the unique feature representation from the data and learns the spatial relationship to prevent misdetection in the SS. In both

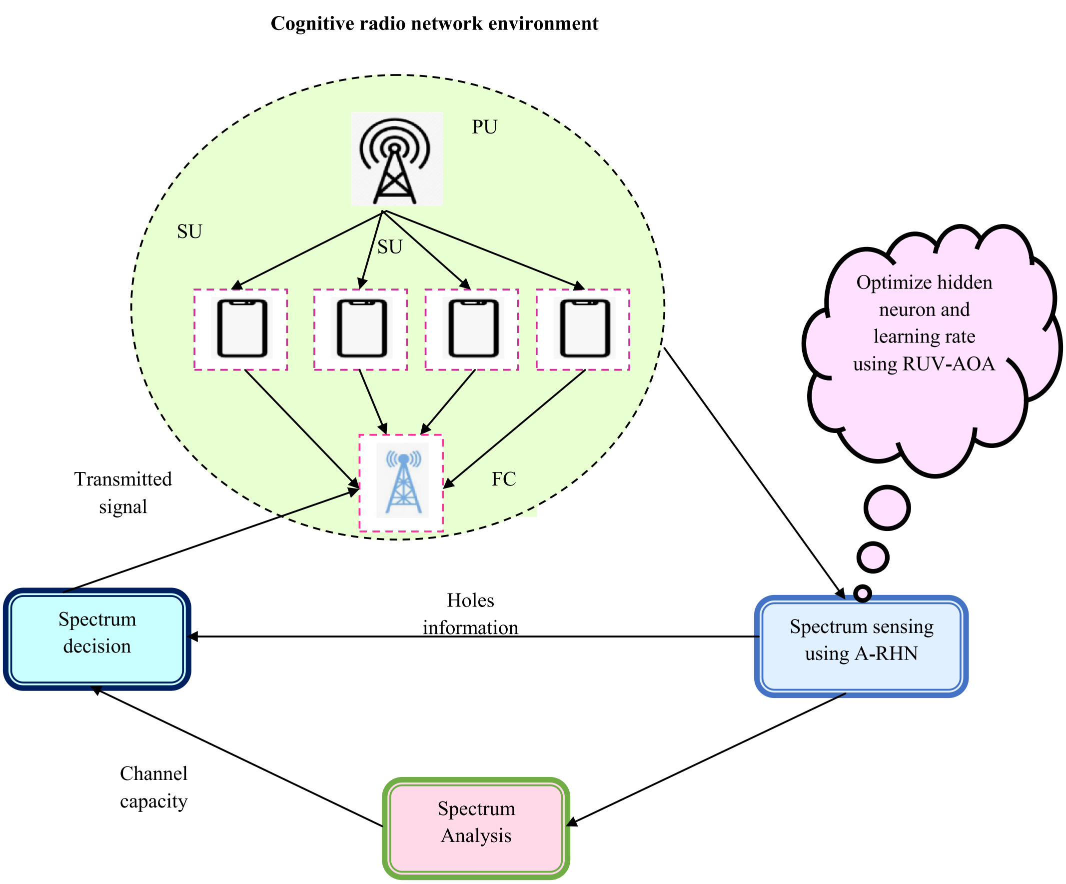

FIGURE 2 | Overall view of the proposed model.

models, the residual connections are added that help to maintain the flow of the gradient within the network to get precise results in the SS. The learning rate and hidden neurons are the parameters of the attention-based autoencoder and multi-scale capsule network that are tuned using the RUV-AOA to maximize the accuracy and minimize the FOR. The A-RHN model enhances the reliability of the SS in the dynamic radio environment. At last, the comprehensive outcome of the proposed model is verified in terms of various experimentation processes.

4.2 | Presented RUV-AOA

Eventually, the SS performance of the A-RHN is improved by tuning the parameters using the RUV-AOA, thereby greatly improving the sensing performance. The RUV-AOA is the most reliable algorithm for enhancing the SS performance of the A-RHN, as it is more adaptable to the radio environment. The RUV-AOA is implemented in the multi-objective optimization, and it is more flexible in the scenario of wireless environment. The suitable optimal solution in the whole optimization process is defined by the RUV-AOA; also, it can also avoid the local optima. The RUV-AOA attains the global optimal solution by exploiting the area near the individual location. Through the RUV-AOA, the parametric alteration of the CR is also attained. The RUV-AOA performs the searching operation to enhance the experience of the individual in the optimization process. The AOA [31] emulates the habitats and natural behavior of the addax for solving engineering problems. The quasi-optimal solution is attained using the AOA. The AOA establishes the balance between exploitation and exploration, and it also performs well in exploration and exploration. The slow convergence and frequently falling into the local optima are the major challenges of the AOA. The unnecessary search efforts of the AOA affect the exploitation capability of the algorithm. The significant potential of this research is to successfully solve the challenges of the AOA by introducing some improvement in the AOA; for this purpose, the random number has been improved concerning the worst, current, and best fitness factors, and it is expressed in Equation (4).

$$s = \frac{er}{rt} - yu \times \frac{1}{er - yu} \tag{4}$$

Here, the improved random number is represented as s, and it is upgraded in Equation (5) of the conventional AOA. The worst fitness is er, the current fitness is rt, and the term yu expresses the best fitness.

$$y_{j,k}^{Q2} = y_{j,k} + (1 - 2s) \cdot \frac{jk_k - ml_k}{u} \tag{5}$$

The new position of the addax j is $y_{j,k}^{Q2}$ and the position of the addax at the dimension k is $y_{j,k}$, the upper and lower limits are jk_k, ml_k, and the current iteration is u. The improved random number in the AOA enhances both exploitation and exploration in the search process. In addition, the unwanted searching process is cut down by the improved random parameter, which prevents both stagnation in the condition of the local optima and premature convergence in the AOA. The pseudocode of the RUV-AOA is given in Algorithm 1.

ALGORITHM 1 | RUV-AOA.

```
Input: Hidden Neuron in AA and MCN w_k^AA, w_u^MCN,
Learning Rate in AA and MCN t_l^AA, t_k^MCN
Output: Optimized Hidden Neuron in AA and
MCN w_k*^AA, w_u*^MCN, Optimized Learning Rate in AA
and MCN t_l*^AA, t_k*^MCN
Set the population size O and iteration u
Develop the initial population
While the termination is not fulfilled
 Determine the objective function
Improve the random number using the Eq.
(5).
 For u = 1toU
   For u = 1toU
     Phase 1: Foraging
     The foraging area of the addax is
     determined.
     The target foraging area of the addax
     is selected.
     The new position of the addax is
     determined and upgraded.
     Phase 2: Digging
     The new position of the addax is
     determined and upgraded.
    End for
  End for
End while
Upgrade the best solution
Stop
```

4.3 | Attention-Based Autoencoder

The AA [32] is made up of an attention mechanism and autoencoder structure for providing excellent results in the SS. The global spatial features of the data are attained by the attention mechanism, and the local features of the data are attained by the autoencoder model for minimizing the dimension of the data. The utilization of the AA addresses the difficulties in retrieving the global spatial features in the data. The relevant attention weight in the structure is used for dynamically learning the features in the input data. Attention mechanisms (AM) are now commonly employed in artificial intelligence. The logical justification for the AM mechanism is to have a tendency to consciously focus on specific aspects of data while eliminating other unimportant information, hence simplifying the detection process. AM enables the model to continuously focus on specific input elements that are useful for efficiently completing the tasks at hand by assigning attention weights to various input parts. Formally stated, AM is the process of translating a query and a collection of key-value pairs into an output, and it is expressed in Equation (6).

$$f = AM(QRY, KY, VLE) \tag{6}$$

Here, the weight is represented as f, and the query, key, and values are represented as QRY, KY, VLE. Under the unsupervised learning paradigm, the autoencoder is a reduced-dimensional model. In order to learn a representation of data that may be utilized to reassemble the given input, its objective is to replicate the input as closely as feasible to the output. Two convolutional layers and one max-pooling layer are used in the encoder portion of the model, and two convolutional layers and one upsampling layer are used in the decoder portion. The input given to the autoencoder is represented as $N_x(\overline{y})$, and the encoder part processes these data to attain the encoded data F.

$$F_{fe} = F\left[N_x(\overline{y})\right] \tag{7}$$

The Mapper is used for mapping the data after the encoding process. The encoded data are decoded using the decoder part.

4.4 | Multi-Scale Capsule Network

The hierarchical features of the input data are exploited by the multi-dimensional capsules in the multi-scale capsule network [33]. One fully connected layer and two convolution layers are available within the shallow structure. The standard convolution layer is the first layer, and the multi-scale capsule encoding is the second layer within the network. The digit layer is located at the end of the structure. The group of neurons in the CapsNet is called as capsules. The orientation and the location of the entity are captured by the direction of the capsule. The probability of the entity's existence is determined by the length of the capsule, and it is given in Equation (8).

$$w_k = \frac{\|t_k\|^2}{1+\|t_k\|^2}\frac{t_k}{\|t_k\|} \tag{8}$$

Thus, the total input is represented as t_k; at the capsule k, the generated capsule is denoted as w_k. The MCN has two stages: Multi-scale feature extraction is used in the initial stage to collect fundamental and semantic information. Linguistic information is extracted by the high-level feature selection procedure, which encompasses the first two layers of the top branch. Medium-level characteristics are extracted using the middle branch's first layer. Without a trainable parameter layer, the bottom branch uses the original features directly. We encode a feature hierarchy into a multi-dimensional primary capsule in the following stage. To encode high-degree, medium-level, and minor characteristics, we take advantage of the final layer between the three branches, generating 4D, 8D, and 12D capsules, respectively. The multifaceted primary capsule is obtained by using three branches. The anticipated vectors are then calculated using various weight matrices in the manner described below:

$$\widehat{v}^1_{k|j} = W_{jk}v^1_j \tag{9}$$

$$\widehat{v}^2_{k|j} = X_{jk}v^2_j \tag{10}$$

$$\widehat{v}^3_{k|j} = V_{jk}v^3_j \tag{11}$$

$$\widehat{v} = concat\left(\widehat{v}^1, \widehat{v}^2, \widehat{v}^3\right) \tag{12}$$

Here, the weight matrices are denoted as X, Y, Z; from the branch l, the primary capsule j is represented as v^l_j. In between the parent capsule k and child capsule j, the predicted vector is denoted as $\widehat{v}^l_{k|j}$, the results of the multiscale capsule encoding is represented as $\widehat{v}$, and the concatenation function is represented by the term *concat*(). The weight between the parent capsule k and the child capsule j is used for information encoding. Dropout renders adjacent hidden units to prevent typical overfitting. Each capsule in CapsNet is a vector, and the dropout must discard a vector instead of specific vector elements. A conventional dropout algorithm can only discard a portion of a capsule; this causes a false recognition by altering the capsule's orientation, which alters the qualities of the capsules.

5 | Proposed A-RHN for Efficient SS and Its Objective Function

5.1 | Network Description of ARHN

The A-RHN combines an attention-based autoencoder with a multi-scale capsule network, for SS in CR networks to handle the growing complexity and dynamic characteristics inherent in wireless communication environments. Conventional SS techniques frequently face difficulties in adapting to fluctuations in signal properties and interference. The A-RHN framework effectively tackles these issues by employing an attention-based autoencoder to emphasize critical features within the spectrum data, thereby improving signal representation and distinction. Furthermore, the integration of a multi-scale capsule network captures hierarchical relationships and contextual details across various scales. This combined strategy not only enhances the accuracy of detecting available spectrum bands but also increases resilience against noise and interference, resulting in more efficient spectrum utilization within CR networks. By harnessing these cutting-edge neural network technologies, the A-RHN seeks to deliver an advanced solution that satisfies the rigorous requirements of contemporary communication systems. In both models, the residual blocks [34] are used to learn the semantic aspects while preserving more information and gradients and assisting it in capturing intricate details. Information can move straight through the network because of residual blocks, which include residual learning methods and skip connections. It also encourages more efficient learning and presentation of input features.

$$G = H(g) + g'_1 + g_{23}'' \tag{13}$$

$$g_{23} = H(g_3) + g'_2 \tag{14}$$

Here, the residual block is g, and the concatenated features are g_{23}, g'_1, and g'_2. In A-RHN, the input is given to both MCN and AA. The results will be obtained by the fusion of features from the two models. The structural illustration of the ARHN is given in Figure 3.

5.2 | Optimal SS Using ARHN

Due to the rise in the number of users in the wireless environment, the availability of the spectrum is scarce in the CR. The vacant spectrum holes of the CR are utilized by another service provider with the help of inbuilt technology in the CR. The complex

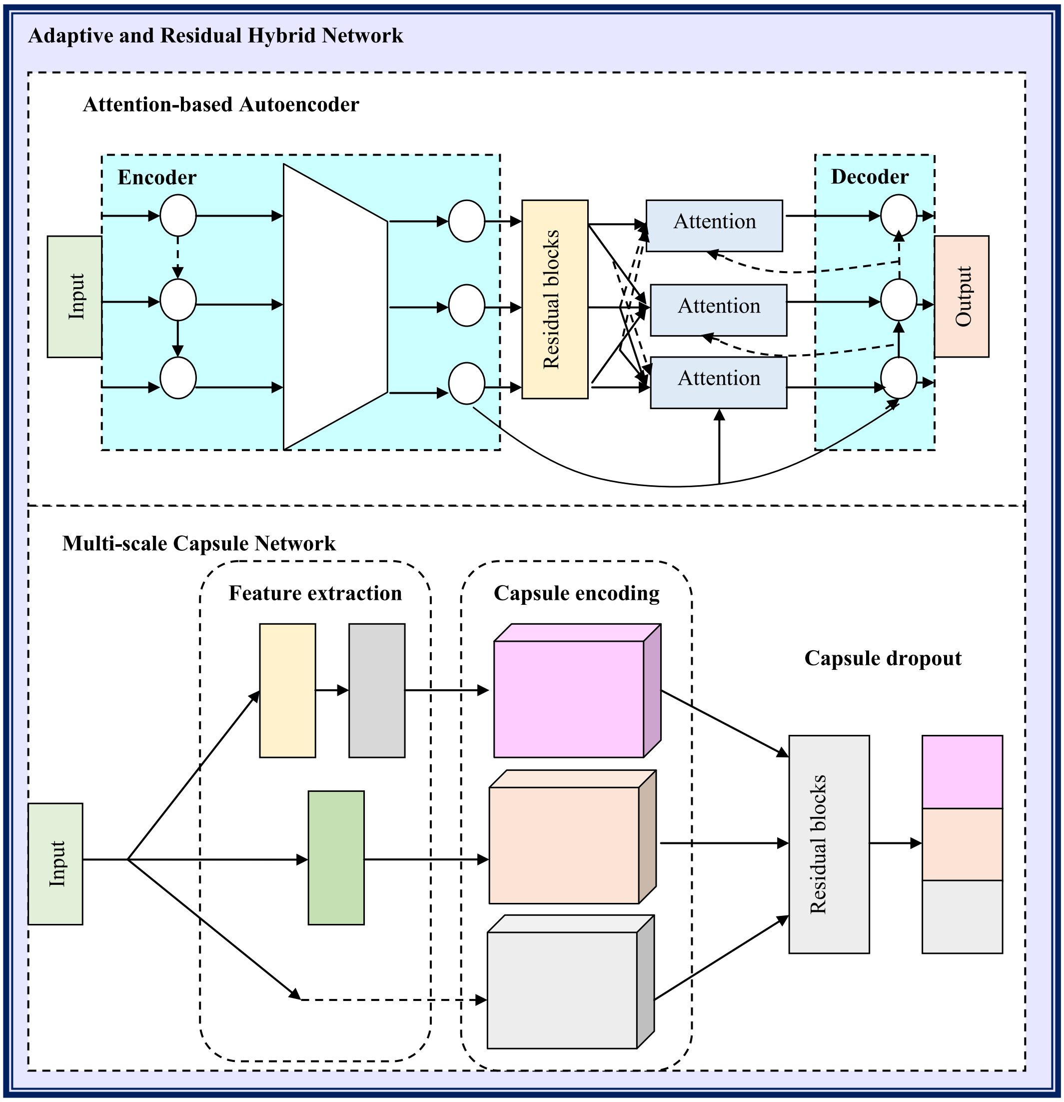

FIGURE 3 | Structural illustration of the ARHN.

relationship in the data is captured using the ARHN. Here, the activity of the PU and the spectrum usage patterns are provided by the capsule mechanism with the CapsNet structure since it can preserve the orientation and spatial features in the input data. The intermediate spectrum behavior and long-term pattern of the PU are captured by the multi-scale framework in this model. While detecting the spectrum in the unpredictable era, the generalization performance of the CapsNet is enhanced, and the transformation in the input data is attained with the help of this structure.

5.2.1 | Integration of Attention Mechanism With Autoencoder

In the CRN platform, the autoencoder mechanism can significantly learn and capture the nonlinear relationships among the nodes to efficiently generate better solutions within a limited labeled data, and also, it is highly suitable for complex radio environments. It has the ability to quickly compress the radio signals, and it is mostly sufficient to train the normal signal patterns for identifying the signals. Yet, it is complex for capturing complex relationships in the data to enhance more computational duration, and it requires more high-dimensional data to generate perfect results. Also, it is more sensitive for efficiently handling limited labeled data to enhance underfitting issues. In order to improvise the performance, the attention mechanism is integrated with autoencoder module to form a new AA mechanism. This integration helps to improve the system's robustness by focusing most essential signal features, resulting better performance in complex channel conditions. AA suppresses the noise and irrelevant information in the input data for analyzing the activity between the PU and SU. The AA retains the important information while reducing the dimension of the input data, so the computational efficiency of the SS is greatly enhanced. In order to improve the AA performance, the multi-scale capsule network is integrated for improving the overall performance.

5.2.2 | Integration of AA With Multi-Scale Capsule Network

The multi-scale capsule network can quickly identify the crucial spectrum patterns while the presence of minimal and higher noise conditions, enabling better feature extraction capabilities to generalize better communication. In the SS performance of the CRN network, the integration of the AA mechanism with the multi-scale capsule network can significantly improve the detection phase by effectively removing the noise and capturing complex spatial-temporal features in diverse network conditions, maximizing better sensing accuracy and robustness. Also, it has the ability to handle vast amounts of input signals for minimizing the overfitting complexities in the training and validation performance. Further, it consumes minimal computational duration for extracting the relevant primary features when processing small and larger volume datasets to improve the optimal accuracy rates. The combination of the AA-MCN approach can develop a novel approach named as ARHN. The ARHN model is robust against noise because it combines the two different models along with the optimization algorithm. First, the synthetically generated data are given to the AA and MCN network where both models can process the input data to provide the two sets of features. These features are averaged to get the final results, which provide the details regarding the available spectrum within the CR. The amount of acceptable spectrum at the transceiver side of the CR is determined using this model, and the presence of the PU is estimated with the help of suggested ARHN-based SS. Here, the information from the environment is collected by the many CR in the SS operation. The cost of the SS operation is very low, and the proposed ARHN added many advantages to the SS operation. The presence of the PU is informed to the nearby cognitive user via the far-away cognitive user. The derivation for the SS using the ARHN in the CR is expressed as follows:

The hidden primary user problem and the probability of a false alarm are greatly reduced by ARHN-based SS, which is used to determine the information broadcast between the cognitive nodes [35]. The proposed ARHN model uses the information provided in the different time slots for SS, and the adaptability of the ARHN model is very high.

The spectrum within the location area is sensed by each SU during the sensing process, and after sensing the SU, the decision has been taken. At the SU, the sampled received signal $Z(o)$ when the PU is active is given in Equation (15).

$$Z(o) = v(o) \tag{15}$$

Else, it is expressed in Equation (16).

$$Z(o) = t(o) + v(o) \tag{16}$$

The signal of the PU is $t(o)$; for the mini slot j, the test statistic $U_j(z)$ is given in Equation (17).

$$U_j(z) = \frac{1}{O_1} \sum_{o=1}^{O_1} \left| z_j(o) \right|^2 \tag{17}$$

$$U(z) = \frac{1}{O_1} \sum_{o=1}^{O_1} h_j U_j(z) \tag{18}$$

At the mini slot j, the weighting factor is represented as $h_j \geq 0$, and the minimum achievable probability of the false alarm Q_e is given in Equation (19).

$$h_j = \frac{\left| i_j \right|^2}{\sqrt{\sum_{j=1}^{N} \left| i_j \right|^4}} \tag{19}$$

Equation (20) expresses the maximum probability of the detection.

$$Max \sum_{j=1}^{N} h_j \left| i_j \right|^2 \tag{20}$$

Equations (21) and (22) show the probability of the false alarm and detection probability.

$$Q_g = R_g\left(C_1 R_g^{-1} Q_e^{-1} \right) + \mathfrak{I} \sqrt{\frac{O}{N}} \sum_{j=1}^{N} \left| i_j \right|^2 \tag{21}$$

$$Q_e = R_e\left(\frac{1}{C_1} R_g^{-1} Q_e'^{1} \right) - \sqrt{\frac{O}{N}} \mathfrak{I} \sum_{j=1}^{N} \left| i_j \right|^2 \tag{22}$$

$$C_2 = \sqrt{1} + \frac{2\mathfrak{I}}{N} \sum_{J=1}^{N} \left| i_j \right|^2 \tag{23}$$

Many nodes are taken into consideration while executing the SS:

$$I_1 : z_j(o) = i_j t(o) + v_j(o) \tag{24}$$

$$I_0 : z_j(o) = v_j(o) \tag{25}$$

$$z(o) = \sum_{j=1}^{N} \frac{ij^*}{\sum_{j=1}^{N} |ij|^2} z_j(o) \tag{26}$$

The hypothesis is equivalently given as follows:

$$I_1 : z(o) = \sqrt{\sum_{j=1}^{N} \left| i_j \right|^2} t(o) + v(o) \tag{27}$$

$$I_0 : z(o) = v(o) \tag{28}$$

$$Q_g = R_g\left(C_1' R_g^{-1} Q_e' \right) + \sqrt{\mathfrak{I} O} \sum_{j=1}^{N} \left| i_j \right|^2 \tag{29}$$

$$C_1' = \sqrt{2\mathfrak{I}} \sum_{J=1}^{n} \left| i_j \right|^2 + 1 \tag{30}$$

The probability of the detection with the probability of a false alarm is given in Equation (31).

$$Q_e = R_e\left(\frac{1}{C_2'} R_e^{-1} Q_e' \right) + \sqrt{\mathfrak{I} O} \sum_{j=1}^{N} \left| i_j \right|^2 \tag{31}$$

$$R_e = \sum_{j=1}^{O} Q_{ej} \left(1 - Q_e \right)^{O-1} \tag{32}$$

$$R_g = \sum_{j=1}^{O} Q_{gj}\left(1 - Q_g\right)^{O-1} \tag{33}$$

Here, the interference level is represented as Q_e, and the CR network's throughput is represented as Q_g. The pictorial illustration of the ARHN-based SS is given in Figure 4.

5.2.3 | Overall Pipeline Process of the Proposed ARHN Method

Initially, the collected synthetic data are given to the SS phase, which contains an adaptive and residual hybrid network. The encoder, residual blocks, attention layer, and decode layer are presented in the attention-based autoencoder mechanism. At first, the encoder layer can effectively compress the gathered synthetic spectrum data into a low-dimensional latent data to recognize and separate the salient features by reducing the noise and irrelevant information from the input data. It has the ability to significantly handle raw complex signal samples within a limited duration to generate a bottleneck vector or latent representation of spectrum data, and it is further fed into the residual block. The residual block can convert the latent representation of spectrum data into image data, and it can optimally reduce the image dimension to learn robust spectrum usage patterns and maximize the accuracy of overall SS performance; thus, it finally generates a set of feature maps. The output (feature map) of residual blocks is given to the attention layers. The attention layer can ultimately assign optimal weights to the input feature maps by focusing and prioritizing the primary features for accurate spectrum sensing, and it

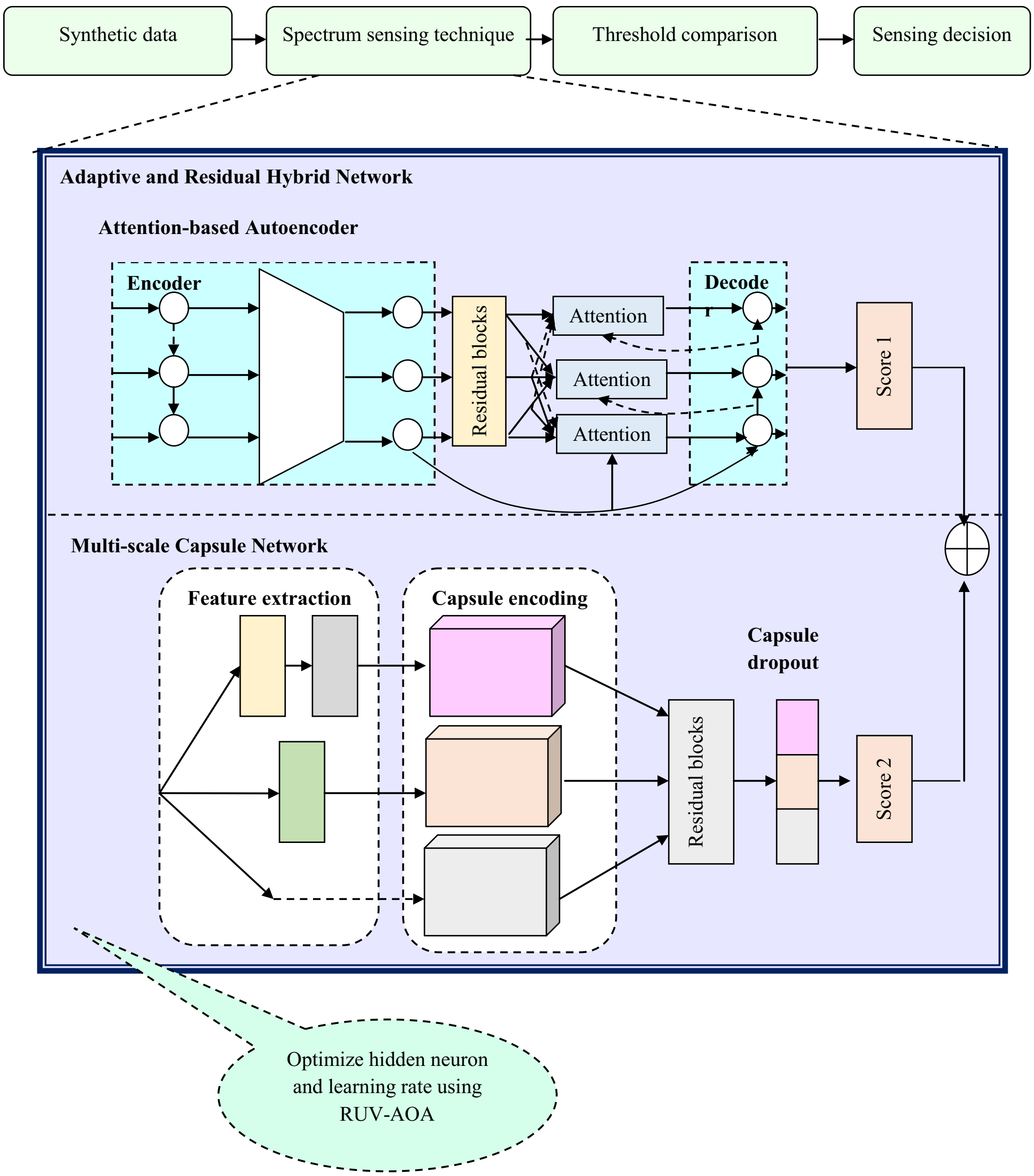

FIGURE 4 | A pictorial illustration of the ARHN-based SS.

generates a weighted feature matrix. Further, a weighted feature matrix can be given to the decoder phase, which helps to reconstruct the original input data from the compressed data by expanding the reduced-dimension feature map to the original dimension of spectral data, and it is represented as Score 1. Moreover, the multi-scale capsule network contains feature extraction, capsule encoding, residual blocks, and capsule dropout layers. In the feature extraction performance in the MCN network, the convolutional layers are utilized to optimally obtain the relevant structural information by extracting the high- and medium-level features. Then, the extracted features are given to the capsule layers, which can encode the input features into vectors that help to identify the presence of complex signals among various frequency bands for minimizing the dimensionality of data. Also, the output of capsule layer can be fed into the residual block, which can ultimately minimize the vanishing gradient and overfitting complexities in the training phase. Also, it can monitor and capture the spectral-spatial features from various scales of input data to provide a multi-scale feature representation for maximizing the generalization ability. Moreover, the spectral-spatial features are given to the capsule dropout layer, which can randomly sett the overall channel to zero in the training phase for improving the robustness by strengthening the entire performance, ensuring better SS phase. The output of the capsule dropout layer (subset of capsules, which are dynamic vector representations) is denoted as Score 2. Then, the output of the AA mechanism (Score 1) and the output of MCN mechanism (Score 2) are concatenated with the help of a summation layer to generate a sensing outcome. Additionally, the optimization phase is held to significantly tune the prescribed parameters of the ARNH network for improving the convergence speed and minimizing the computational complexity in an efficient manner. The outcome of sensing result can further be given to the threshold comparison phase to contrast the features of received signal with the predefined threshold for validating the presence of PU, and it generates a binary decision outcome. Then, the binary decision outcome is given to the sensing decision phase, which can significantly monitor and capture the presence and absence of PU by ultimately recognize the received signal to enhance better decision-making performance.

5.3 | Objective Function

The parameters of the ARHN, such as learning rate and hidden neuron, are tuned using the RUV-AOA for enhancing the accuracy and minimizing the FOR. The optimization of the above parameters reduces the training time and navigates the training process to get precise results. In addition, the underlying patterns and the relationship between the input data are captured using the ARHN by tuning the parameters using the RUV-AOA. The objective function of the RUV-AOA-ARHN-based SS is given in Equation (34).

$$ty = \underset{\left\{t_{l*}^{AA}, t_{k*}^{MCN}, w_{k*}^{AA}, w_{u*}^{MCN}\right\}}{\arg\min} \left(\frac{1}{Acr} + FOR\right) \tag{34}$$

Thus, the objective function is represented as ty, the optimized hidden neuron in AA and MCN is denoted as $w_{k*}^{AA}, w_{u*}^{MCN}$, and they lie in $[5, 255]$. Optimized learning rate in AA and MCN is represented as $t_{l*}^{AA}, t_{k*}^{MCN}$ and stuck in $[0.01, 0.99]$. The accuracy and FOR are determined as follows:

$$FOR = \frac{lp}{lp + az} \tag{35}$$

$$Acr = \frac{aq + az}{aq + az + lm + lp} \tag{36}$$

The factors aq, az are true positive and negative, respectively, and the term lm, lp expresses the false positive and negative correspondingly.

6 | Simulation Results and Discussion

6.1 | Simulation Environment

Python simulations were used to confirm the theoretical finding of the proposed SS model. During the simulation, the conventional models such as gorilla troops optimizer (GTO) [36], border collie optimization (BCO) [37], red-billed blue magpie optimizer (RBMO) [38], AOA [31], and the ODL-MUDSS [18], LSTM-SS [20], AE [32], and CapsNet [33] were adopted to reveal the performance of the developed SS model.

6.2 | Simulation Metrics

The "F1score, False Discovery Rate (FDR), False Negative Rate (FNR), False positive rate (FPR), Mathews Correlation Coefficient (MCC), Negative Predictive Value (NPV), Precision Pr, Sensitivity *sen*, and Specificity *spc*" are used for validating the performance of the developed model.

$$F1score = \frac{2aq + az}{2aq + lm + lp} \tag{37}$$

$$FDR = \frac{lm}{aq + lm} \tag{38}$$

$$FNR = \frac{lp}{aq + lp} \tag{39}$$

$$FPR = \frac{lm}{lm + lp} \tag{40}$$

$$NPV = \frac{az}{az + lp} \tag{41}$$

$$\Pr = \frac{aq}{aq + lm} \tag{42}$$

$$sen = \frac{aq}{aq + lp} \tag{43}$$

$$spc = \frac{az}{az + lm} \tag{44}$$

6.3 | Comparative Analysis of the Proposed Approach

Under the diverse epoch count values, the sensing performance of the developed ARHN with other existing models is given in Figure 5. The results of the proposed RUV-AOA-ARHN attain better sensing gain compared to ODL-MUDSS, LSTM-SS, AE, and CapsNet models since the suggested model is the hybrid network that leverages the capability of both models prevent the missed detection in the SS. In the 50th epoch, the sensing performance of the GTO-ARHN and RBMO-ARHN is nearly the same in terms of accuracy metric, so the accurate detection capability of both models is slightly lower than the proposed RUV-AOA-ARHN. Moreover, the sensing capability of the RUV-AOA-ARHN is a higher precision of 96.7 over the prior models like ODL-MUDSS, LSTM-SS, AE, and CapsNet. From the

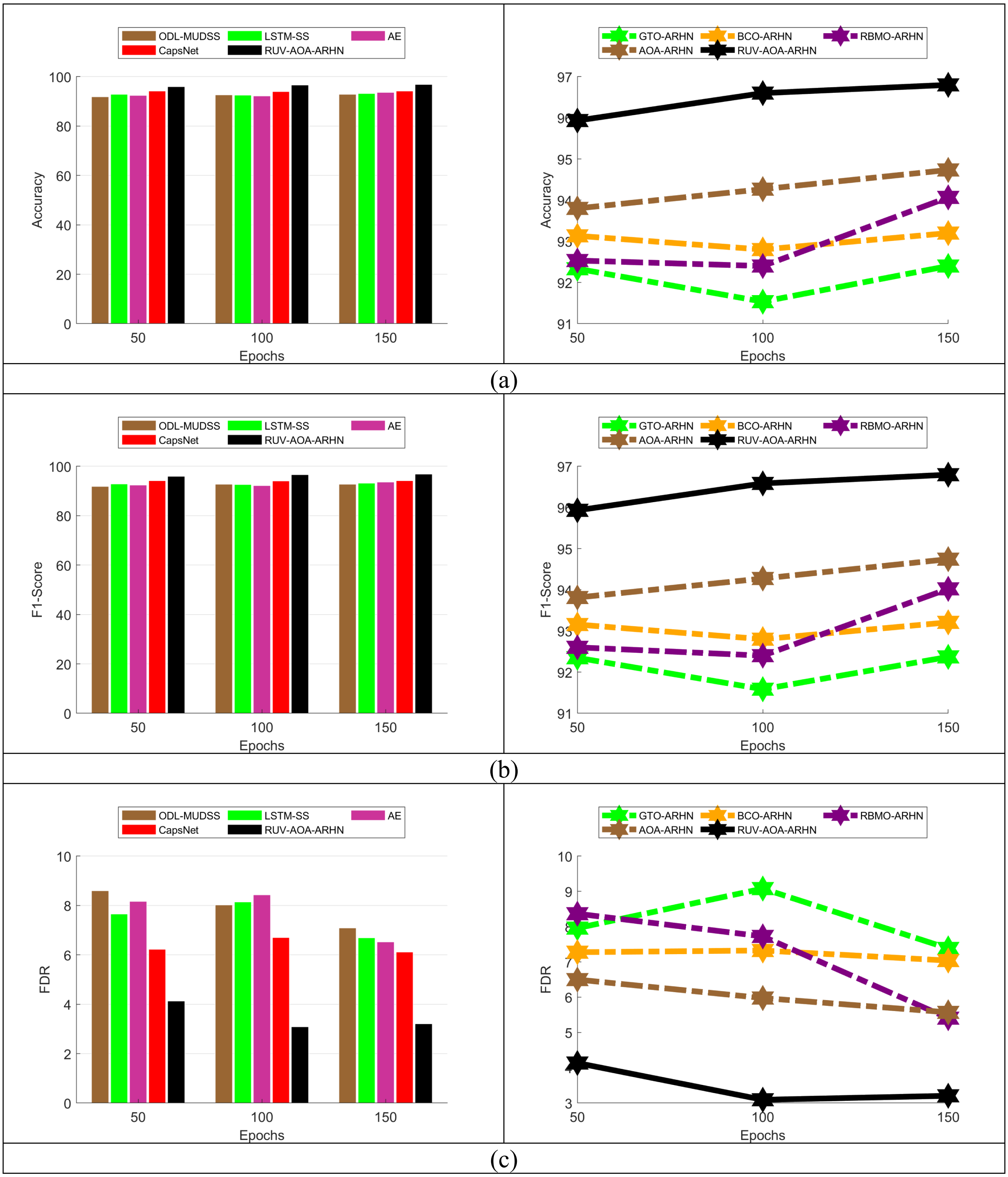

FIGURE 5 | Comparison of the proposed hybrid deep learning-based SS for (a) accuracy, (b) F1score, (c) FDR, (d) FNR, (e) FPR, (f) NPV, (g) precision, (h) sensitivity, and (i) specificity.

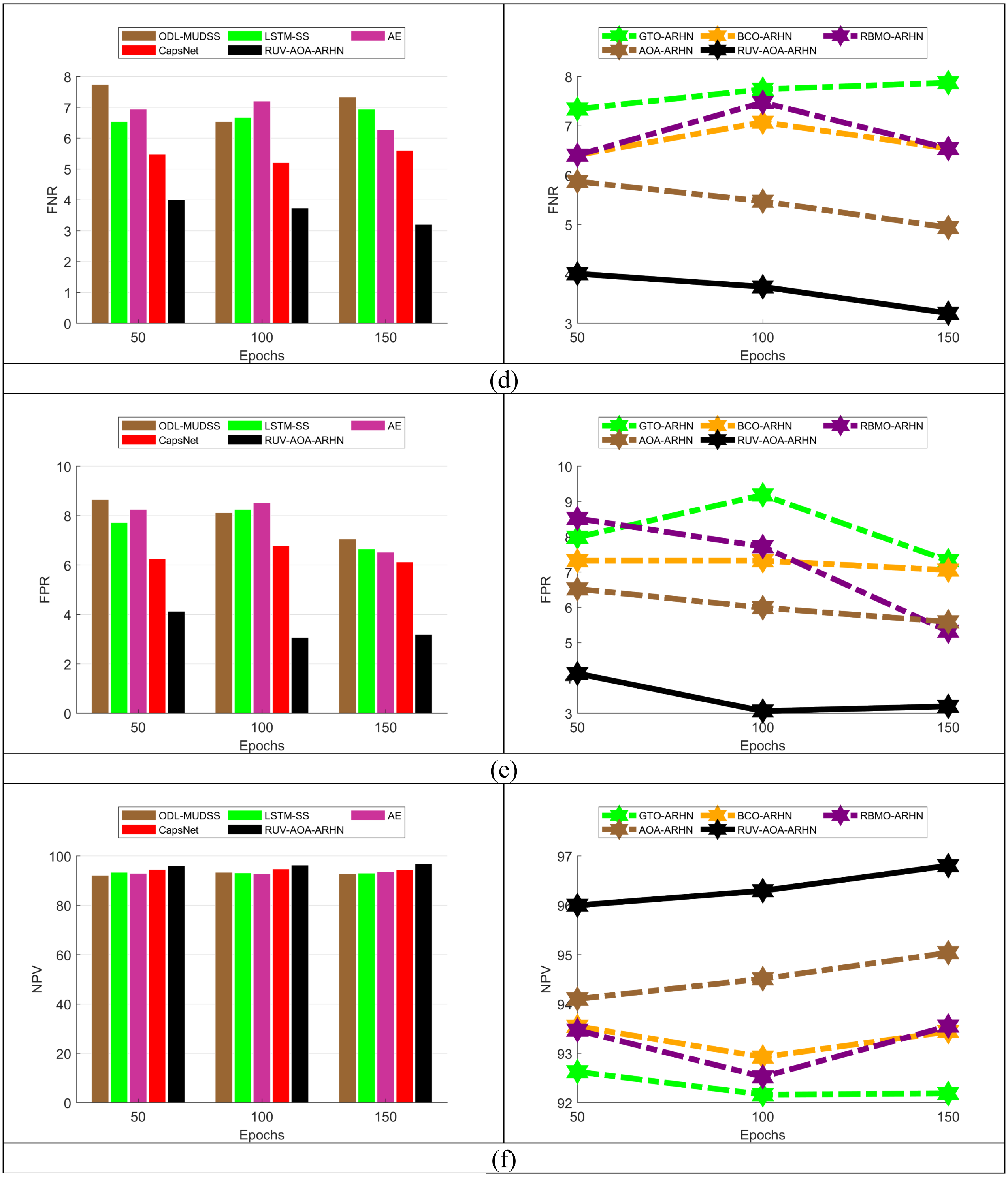

FIGURE 5 | Continued

results, it can be observed that the proposed RUV-AOA-ARHN significantly provides better detection results even in all epoch counts, which ensures the high sensing probability of the proposed model. The main reason is that the suggested RUV-AOA-ARHN combines the two models along with the residual blocks that can optimize sensing node collection and enhance the quality of the sensing channel.

6.4 | Convergence Analysis

The convergence analysis is conducted to show the performance of the RUV-AOA in the sensing operation. It is evident from Figure 6 that the proposed RUV-AOA-ARHN model converges from the initial stage of the iteration without stagnating at the local optima. The flat line shown in the black color

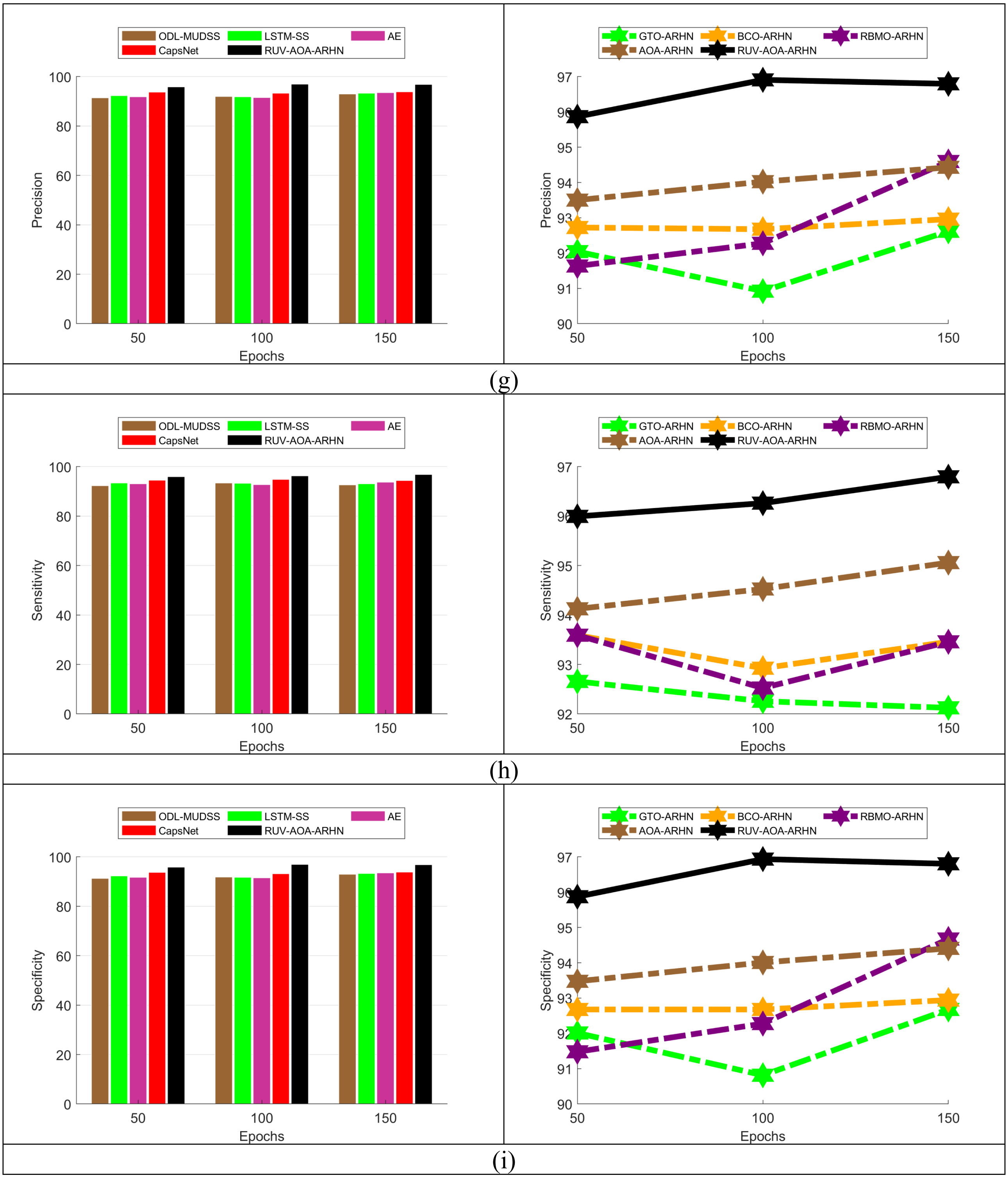

FIGURE 5 | Continued

proved that the proposed RUV-AOA-ARHN has higher convergence capability and reaches the global optima solution within the minimum iteration. The convergence results of the RUV-AOA-ARHN verify whether the suggested system reaches the maximum convergence to the point of interest. The RUV-AOA-ARHN follows the collective behavior of the addax to provide intelligent solutions to optimization issues.

6.5 | Performance Evaluation of the Proposed Approach

In this section, the performance of the developed RUV-AOA-ARHN, measured in terms of various performance indices, is given in Table 2. The accuracy values of the ODL-MUDSS, LSTM-SS, AE, and CapsNet were adopted for calculating the efficiency of the proposed RUV-AOA-ARHN in the SS operation. The accuracy of the proposed RUV-AOA-ARHN is 96.8, and it provides a noticeable improvement over the conventional models since they reach the 92.8, 93.2, 93.6, and 94.133 accuracy value in SS operation. Moreover, the proposed RUV-AOA-ARHN attained a higher precision value compared to the ODL-MUDSS, LSTM-SS, AE, and CapsNet, which confirms the effective sensing capability of the proposed RUV-AOA-ARHN in the SS. From the numerical results, it has been evident that the proposed RUV-AOA-ARHN particularly excels in detecting the presence or absence of the SU in the CR leading to the enhancement of the transmission capability in the CR. Moreover, the suggested RUV-AOA-ARHN is also used for handling the spectrum sacristy issues and provides the energy-efficient and optimal solution.

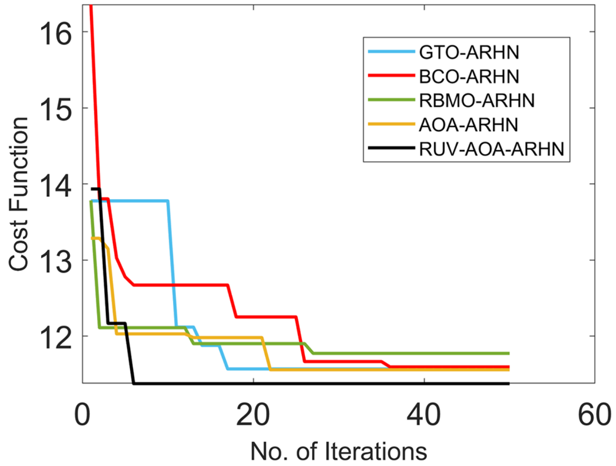

FIGURE 6 | Convergence analysis of the proposed SS model over other algorithms.

6.6 | Computational Complexity Validation of the Proposed Approach

Table 3 shows the proposed approach's computational complexity validation with various conventional methods. This analysis helps to optimize resource utilization and learn the scalability of the developed method to enable effective performance. It helps to significantly select the hyperparameters to generate

TABLE 2 | Performance evaluation of the proposed model over other approaches.

Algorithms					
Terms	**GTO-ARHN [36]**	**BCO-ARHN [37]**	**RBMO-ARHN [38]**	**AOA-ARHN [31]**	**RUV-AOA-ARHN**
Accuracy	92.4	93.2	94.1	94.7	96.8
Sensitivity	92.1	93.5	93.5	95.1	96.8
Specificity	92.7	92.9	94.7	94.4	96.8
Precision	92.6	93.0	94.6	94.4	96.8
FPR	7.3	7.1	5.3	5.6	3.2
FNR	7.9	6.5	6.5	4.9	3.2
NPV	92.2	93.4	93.6	95.0	96.8
FDR	7.4	7.0	5.4	5.6	3.2
F1-Score	92.4	93.2	94.0	94.7	96.8
MCC	84.8	86.4	88.1	89.5	93.6
Methods					
Terms	**ODL-MUDSS [18]**	**LSTM-SS [20]**	**AE [32]**	**CapsNet [33]**	**RUV-AOA-ARHN**
Accuracy	92.8	93.2	93.6	94.1	96.8
Sensitivity	92.7	93.1	93.7	94.4	96.8
Specificity	92.9	93.3	93.5	93.9	96.8
Precision	92.9	93.3	93.5	93.9	96.8
FPR	7.1	6.7	6.5	6.1	3.2
FNR	7.3	6.9	6.3	5.6	3.2
NPV	92.7	93.1	93.7	94.4	96.8
FDR	7.1	6.7	6.5	6.1	3.2
F1-score	92.8	93.2	93.6	94.1	96.8
MCC	85.6	86.4	87.2	88.3	93.6
Accuracy	92.8	93.2	93.6	94.1	96.8

TABLE 3 | Computational complexity of the proposed model over other approaches.

Model	Training time (s)	Inference time (ms)	Memory (MB)	Parameters	Space complexity	Parameter definition
ODL-MUDSS [18]	49.3	15.2	290	1,200,000	$O(n^2) + O(k^*d)$	n: Number of samples k: Number of dictionary elements/clusters d: Latent dimension
LSTM-SS [20]	45.7	9.8	160	500,000	$O(n^*t) + O(h^2)$	t: Sequence length (time steps) h: Hidden state size
AE [32]	42.5	6.1	180	300,000	$O(n^*d) + O(d^2)$	d: Latent dimension
CapsNet [33]	50.0	18.4	330	2,000,000	$O(n^{2*}r^2) + O(r^3)$	r: Capsule dimension/ routing iterations
RUV-AOA-A-RHN	40.2	5.4	120	1,000,000	$O(n^*d) + O(\log\ n)$	d: Latent/hidden dimension

better trade-offs among resource usage and performance, leading to faster training and minimizing the inference time. Here, the proposed approach has a minimal training time of 40.2 (s) than the conventional approaches to effectively enhance the SS performance in CRN network in an efficient manner. Also, the designed approach has a better space complexity rate, which can improve the feature extraction and optimization performance in the training phase to maximize the detection accuracy and robustness.

7 | Conclusion

In this research, a deep learning model was proposed for SS in the CR. In this system, the A-RHN was proposed by combining the AA and MCN for precisely detecting the presence or absence of the SU within the CR. In addition, the data required for the SS is synthetically generated, and these synthetically generated data enhance the training capacity of the A-RHN. The unused spectrum in the CR was detected by this model. The sensing performance of the proposed scheme over the other models was confirmed by the simulation process. The accuracy of the proposed RUV-AOA-ARHN was 96.8, and it provides a noticeable improvement over the conventional models like ODL-MUDSS, LSTM-SS, AE, and CapsNet since they reached 92.8, 93.2, 93.6, and 94.133 accuracy in SS operation. From the results, the effectiveness of the proposed model in the SS was confirmed. Future work will focus on investigating the scalability of the proposed model with a large network and a huge number of CR devices. The probability of a false alarm will be further reduced using the ensemble model.

7.1 | Limitations

The proposed approach can generate better outcomes in the evaluation phase, yet it needs a high sampling rate and high-speed signal processors for providing the efficient, reliable, and accurate wideband SS with low complexity and minimal computation cost. The proposed approach does not have the probability for detecting and sensing the weak signals to enhance the impact of harmful interference, resulting in poor detection performance. It is complex for selecting and keeping the prior knowledge and appropriate number of measurements to the estimation of sparsity level of a wideband signal in the dynamic network environments. In the evaluation phase, the proposed method takes more recovery time while the utilization of large-scale datasets and it is hard to accurately differentiate a faded and shadowed primary signal.

7.2 | Future Work

In future, the multiple-input multiple-output (MIMO) system will be integrated into the proposed approach to improve the performance by determining the availability of the frequency channel; also, it helps to increase the probability of detection and reduce the false-alarm. The modern pre-processing approaches will be concentrated in upcoming works to optimally recognize and mitigate the faded and shadowed signals by extracting the essential information without any information loss. In future work, the transformer-based model will be considered to improve the spectrum efficiency by analyzing the delay and throughput in the CRN network. Moreover, the time-domain method will be introduced to solve the issues of computational problems; thus, it helps to enhance the SS performance in the CRN system.

Conflicts of Interest

The authors declare no conflicts of interest.

Data Availability Statement

Data sharing is not applicable to this article as no datasets were generated or analyzed during the current study.

References

1. M. T. Ahmed, M. Haque, Y. Sugiura, and T. Shimamura, "Machine Learning Approach to Energy Detection Based Spectrum Sensing for

Cognitive Radio Networks," *IEEJ Transactions on Electrical and Electronic Engineering* 20 (2025): 910–919.

2. K. Wang, Y. Chen, D. Bo, and S. Wang, "A Novel Multi-User Collaborative Cognitive Radio Spectrum Sensing Model: Based on a CNN-LSTM Model," *PLoS ONE* 20, no. 1 (2025): e0316291.

3. H. A. Shinde and S. Garg, "Analysis of Hybrid Spectrum Sensing in Cognitive Radio Using Hybrid Approaches," *Komunikácie* 27, no. 1 (2025): 1–10, https://doi.org/10.26552/com.C.2025.003.

4. A. O. A. Salam, R. E. Sheriff, S. R. Al-Araji, K. Mezher, and Q. Nasir, "Adaptive Spectrum Sensing in Cognitive Radio Employing Multitaper Method and Higher-Order STBC Techniques," *Engineering Science and Technology* 6 (2025): 1–21.

5. Y. Xu, Y. Li, and T. Q. Quek, "RIS-Enhanced Cognitive Integrated Sensing and Communication: Joint Beamforming and Spectrum Sensing," *IEEE Journal on Selected Areas in Communications* 43 (2025): 795–810.

6. A. Kumar, "Spectrum Sensing Beyond 5G System: Deep Learning and Conventional Techniques Analysis," *Multimedia Tools and Applications* 84 (2025): 1–24.

7. M. Mahvash, N. Moghim, M. Mahdavi, M. Amiri, and S. Shetty, "Blockchain-Inspired Trust Management in Cognitive Radio Networks With Cooperative Spectrum Sensing," *Pervasive and Mobile Computing* 106 (2025): 101999.

8. S. D. Shamsi, A. S. H. M. Ali, and W. D. Shamsi, "Hybrid Cooperative Spectrum Structured (HCSS) Approach for Adaptive Routing in Cognitive Radio Ad Hoc Networks," *Mesopotamian Journal of CyberSecurity* 5, no. 1 (2025): 23–38.

9. E. V. Sood and E. M. Singh, "Spectrum Utilization by Using Cognitive Radio Technology," *Communications* 14 (2025): 2110is.

10. C. Ukpong, O. Udeme, E. Idowu-Bismark, et al., "Deep Reinforcement Learning Agents for Dynamic Spectrum Access in Television Whitespace Cognitive Radio Networks," *Scientific African* 27 (2025): e02523.

11. D. Yildiz and S. Demirci, "A Survey of Localization in Cognitive Radio Sensor Networks: An Algorithmic Perspective," in *5G and 6G Enhanced Broadband Communications*, vol. 151 (IntechOpen, 2025).

12. M. Gupta, A. S. Shekhar, and K. Kumar, "RORA: Reinforcement Learning Based Optimal Distributed Resource Allocation Strategies in Vehicular Cognitive Radio Networks for 6G," *Vehicular Communications* 52 (2025): 100882.

13. J. Ukachukwu and E. C. Ashigwuike, "Optimization of Signal to Noise Ratio and Power Consumption of Cognitive Radio Systems Using Enhanced PSO Algorithm," *ATBU Journal of Science, Technology and Education* 12, no. 4 (2025): 273–281.

14. Z. Song, X. Zhang, Z. Chen, R. Tafazolli, and Y. Gao, "GBSense: A GHz-Bandwidth Compressed Spectrum Sensing System," *IEEE Transactions on Circuits and Systems I: Regular Papers* 72 (2025): 4912–4924, https://doi.org/10.48550/arXiv.2410.11495.

15. S. Sunkara and N. R. Banavathu, "Optimal M-out-of-S Rule for Asynchronous Cooperative Sensing in Heterogeneous Cognitive Radio Networks," *IEEE Wireless Communications Letters* 14 (2025): 1079–1083.

16. L. Arcangeloni, E. Testi, and A. Giorgetti, "Leveraging Bayesian Factor Analysis for Cooperative Wideband Spectrum Sensing," *IEEE Transactions on Cognitive Communications and Networking* 11 (2025): 3174–3187.

17. B. Wang, Y. Zhang, F. Chu, G. Ding, and R. Xu, "Analysis and Optimization of UAV-Assisted Covert Communications in Interweave Cognitive Radio Networks," *IEEE Transactions on Cognitive Communications and Networking* 11 (2025): 3188–3201.

18. L. Almuqren, M. Maray, F. A. Alotaibi, A. Alzahrani, A. Mahmud, and M. Rizwanullah, "Optimal Deep Learning Empowered Malicious User Detection for Spectrum Sensing in Cognitive Radio Networks," *IEEE Access* 12 (2024): 35300–35308.

19. H. Kaschel, K. Toledo, J. T. Gómez, and M. J. F.-G. García, "Energy-Efficient Cooperative Spectrum Sensing Based on Stochastic Programming in Dynamic Cognitive Radio Sensor Networks," *IEEE Access* 9 (2021): 720–732.

20. B. Soni, D. K. Patel, and M. López-Benítez, "Long Short-Term Memory Based Spectrum Sensing Scheme for Cognitive Radio Using Primary Activity Statistics," *IEEE Access* 8 (2020): 97437–97451.

21. H. S. Fouda and M. M. Fouda, "Three Novel Statistical Tests-Inspired Spectrum Sensing Techniques for Cognitive Radio," *IEEE Communication Society* 5 (2024): 7041–7056.

22. M. S. Miah, M. Schukat, and E. Barrett, "A Throughput Analysis of an Energy-Efcient Spectrum Sensing Scheme for the Cognitive Radio-Based Internet of Things," *Journal of Wireless Communications and Networking* 2021 (2021): 201.

23. H. Ye and J. Jiang, "Optimal Linear Weighted Cooperative Spectrum Sensing for Clustered-Based Cognitive Radio Networks," *Journal of Wireless Communications and Networking* 2021 (2021): 84.

24. E. Ezhilarasi and J. C. Clement, "Robust Cooperative Spectrum Sensing in Cognitive Radio Blockchain Network Using SHA-3 Algorithm," *Blockchain: Research and Applications* 5 (2024): 100224.

25. E. V. Vijay and K. Aparna, "Deep Learning-CT Based Spectrum Sensing for Cognitive Radio for Proficient Data Transmission in Wireless Sensor Networks," *e-Prime Advances in Electrical Engineering, Electronics and Energy* 9 (2024): 100659.

26. J. Yao, M. Jin, T. Wu, M. Elkashlan, C. Yuen, and K. Wong, "FAS-Driven Spectrum Sensing for Cognitive Radio Networks," *IEEE Internet of Things Journal* 12, no. 5 (2025): 6046–6049.

27. V. Roopa and H. S. Pradhan, "Deep Learning Based Intelligent Spectrum Sensing in Cognitive Radio Networks," *IETE Journal of Research* 70, no. 12 (2024): 8425–8445.

28. A. Taherpour, A. Taherpour, T. Khattab, and X. Wang, "Large Array Antenna Spectrum Sensing in Cognitive Radio Networks," *IEEE Transactions on Cognitive Communications and Networking* 11, no. 2 (2025): 1119–1132.

29. C. Ambhika, "Discrimination of Primary User Emulation Attack on Cognitive Radio Networks Using Machine Learning Based Spectrum Sensing Scheme," *Wireless Networks* 30 (2024): 3135–3147.

30. S. K. Mochigar and R. U. Matad, "Improved Quantum Inspired Evolution Algorithm With ResNet50 for Spectrum Sensing in Cognitive Radio Networks," *Bulletin of Electrical Engineering and Informatics* 14, no. 1 (2025): 1–10.

31. T. Hamadneh, K. Kaabneh, O. Alssayed, et al., "Addax Optimization Algorithm: A Novel Nature-Inspired Optimizer for Solving Engineering Applications," *International Journal of Intelligent Engineering & Systems* 17, no. 3 (2024): 732–743.

32. J. Cui, L. Bai, X. Zhang, Z. Lin, and Q. Liu, "The Attention-Based Autoencoder for Network Traffic Classification With Interpretable Feature Representation," *Symmetry* 16 (2024): 589.

33. C. Xiang, L. Zhang, Y. Tang, W. Zou, and C. Xu, "MS-CapsNet: A Novel Multi-Scale Capsule Network," *IEEE Signal Processing Letters* 25, no. 12 (2018): 1850–1854.

34. Q. Y. Hu, W. Zhou, X. Peng, et al., "DRANet: A Semantic Segmentation Network for Chinese Landscape Paintings," *Digital Signal Processing* 147 (2024): 104427.

35. R. Deka, S. Chakraborty, and J. S. Roy, "Optimization of Spectrum Sensing in Cognitive Radio Using Genetic Algorithm," *Facta Universitatis, Series: Electronics and Energetics* 25, no. 3 (2012): 235–243.

36. B. Abdollahzadeh, F. S. Gharehchopogh, and S. Mirjalili, "Artificial Gorilla Troops Optimizer: A New Nature-Inspired Metaheuristic Algorithm for Global Optimization Problems," *International Journal of Intelligent Systems* 36, no. 10 (2021): 5887–5958.

37. T. Dutta, S. Bhattacharyya, S. Dey, and J. Platos, "Border Collie Optimization," *IEEE Access* 8 (2020): 109177–109197.

38. A. A. El-Fergany and A. M. Agwa, "Red-Billed Blue Magpie Optimizer for Electrical Characterization of Fuel Cells With Prioritizing Estimated Parameters," *Technologies* 12, no. 9 (2024): 156.